Inorganica Chimica Acta 363 (2010) 3208–3213

Contents lists available at ScienceDirect

Inorganica Chimica Acta

journal homepage: www.elsevier.com/locate/ica

Synthesis, spectroscopic and structural characterization of the high-spin Fe(II) cyanato-*N* and thiocyanato-*N* “picket fence” porphyrin complexes

Mondher Dhifet [a], Mohamed Salah Belkhiria [a], Jean-Claude Daran [b], Charles E. Schulz [c], Habib Nasri [a,*]

[a] Laboratoire de physico-chimie des matériaux, Faculté des Sciences de Monastir, Avenue de l’Environnement, 5019 Monastir, Tunisia
[b] Laboratoire de Chimie de Coordination CNRS UPR 8241, 205 Route de Norbone, 31077 Toulouse, Cedex 04, France
[c] Department of Physics, Knox College, Galesburg, IL 61401, USA

ARTICLE INFO

Article history:
Received 2 May 2010
Received in revised form 20 May 2010
Accepted 27 May 2010
Available online 2 June 2010

Keywords:
Cyanato complex
Thiocyanato complex
Iron(II) porphyrin
Structural studies
Mössbauer spectroscopy

ABSTRACT

Two new iron(II) five-coordinated porphyrin complexes [Na(2,2,2-crypt)] [Fe^{II}(TpivPP)(NCO)] (**1**) (TpivPP = α,α,α,α-tetrakis(*o*-pivalamidophenyl) porphyrin known as picket fence porphyrin and 2,2,2-crypt is the cryptand-222) and [K(2,2,2-crypt)][Fe^{II}(TpivPP)(NCS)] (**2**) have been prepared and characterized. The UV–Vis and IR spectroscopic data are consistent with a cyanato-*N* and thiocyanato-*N* ferrous porphyrinates. The Mössbauer data and the X-ray structural analysis indicate that the Fe(II) cation in **1** and **2** is high-spin ($S = 2$) and has the $(d_{xy})^2(d_{xz})^1(d_{yz})^1(d_{z^2})^1(d_{x^2-y^2})^1$ ground state electronic configuration.

For complex **1**, the average equatorial iron-pyrrole N bond length ($Fe–N_p = 2.120(2)$ Å), the distance between the iron and the 24-atom mean plane of the porphyrin ring ($Fe–P_C = 0.6805(7)$ Å) and the distance between the iron and the plane made by the four pyrrole nitrogens ($Fe–P_N = 0.5923(12)$ Å) are longer than those of complex **2** and similar five-coordinated Fe(II) high-spin porphyrinates. This is probably due to the significant electronic repulsion of the $d_{x^2-y^2}$ and d_{xy} orbitals by the negative charge of the pyrrole N atoms in case of **1**.

1. Introduction

Understanding how small molecules, such as NO, CO, halides or pseudo-halides (RNC, CN^-, N_3^-, SCN^-, OCN^-, ...) bind to the iron in hemoproteins has been and continues to be a topic of considerable interest [1]. In principle, single-crystal X-ray crystallographic studies of proteins should enable a determination of the local geometries of metal–ligand interactions, but the relatively limited resolution of protein crystal structure has resulted in some controversies as to the actual geometries involved. Iron(II) synthetic porphyrin complexes have been successfully used for many decades as models for hemoproteins.

It has been shown that high-spin Fe(II) porphyrins can be divided into classes having two different electronic configurations [2]. Derivatives type $[Fe^{II}(Porph)(X)]^-$ (Porph = porphyrin and X is a monodentate anionic weak field ligand) have configuration, $(d_{xy})^2(d_{xz})^1(d_{yz})^1(d_{z^2})^1(d_{x^2-y^2})^1$ whereas complexes of type [Fe^{II}(Porph)$(L)_2$] (L is a monodentate neutral σ-donor ligand) have the $(d_{xy})^2(d_{xz})^1(d_{yz})^1(d_{z^2})^1(d_{x^2-y^2})^1$ ground state configuration. This division into two groups is manifested in the molecular structures: complexes with the former electronic configuration have significantly larger iron displacement (~0.18 Å larger) and equatorial $Fe–N_p$ bonds (~0.04 Å longer) than those with the second type of electronic configuration. On the other hand, the first type of high-spin iron(II) porphyrinates presents large positive quadrupole splitting ΔE_q (3.50–4.36 mm/s) while high-spin iron(II) species such as [Fe^{II}(TPP)(2-MeHIm)] (TPP = tetraphenylporphyrin) [2] show negative ΔE_q values in the −1.94 to −2.44 mm/s range.

To date, there are no X-ray molecular structures of an iron(II) cyanato or thiocyanato porphyrin species reported in the literature and especially noteworthy is the very small number of published structural studies on iron-cyanato complexes.

In order to gain more insight into the nature of stereochemical and electronic structure of high-spin Fe(II) porphyrin species, the synthesis, spectroscopic and structural properties of two new five-coordinate Fe^{2+} picket fence porphyrin (TpivPP) complexes with the cyanate and thiocyanate ions as axial ligands are reported here.

The use of picket fence porphyrin for the characterization of ferrous porphyrinates is directly related to the fact that small anionic ligands, as shown by molecular structures [3], are in all cases bound to the iron(II) by the pocket side of the protected porphyrin which avoids the auto-oxidation of the iron(II) species to the iron(III) μ-oxo-porphyrin complex.

2. Experimental

2.1. General

The cryptand-222 was recrystallized from toluene, dried under vacuum and stored under argon in the dark. Toluene and hexanes

---

* Corresponding author. Tel.: +216 73 500 280; fax: +216 73 500 278.
E-mail address: hnasri1@gmail.com (H. Nasri).

0020-1693/$ - see front matter © 2010 Elsevier B.V. All rights reserved.
doi:10.1016/j.ica.2010.05.058

were distilled from their sodium-benzophenone solution under a nitrogen atmosphere. NaOCN and KSCN salts were recrystallized twice from hot distilled water, dried overnight at about 80 °C and stored under argon. Chlorobenzene was purified by washing with sulfuric acid and distilled over P_2O_5. All other reagents and solvents employed were commercially available and were used as received without further purification. All reactions and manipulations for the preparation of the Fe(II) porphyrin derivatives were carried out under argon using a double-manifold vacuum line, Schlenkware and cannula techniques.

UV–Vis spectra were recorded on a Shimadzu UV-2401 spectrometer and Fourier-transformer IR data on a Shimadzu FTIR-8400 spectrometer. Mössbauer measurements were performed on a constant acceleration spectrometer from 25 to 100 K with an optional small field (Knox College). Single crystal X-ray diffraction data were collected by Bruker APEXII CCD diffractometer.

2.2. Synthesis of [Na(2,2,2-crypt)][Fe^{II}(TpivPP)(NCO)](**1**)

[Fe^{III}(TpivPP)(SO_3CF_3)(H_2O)] [4] (100 mg, 0.081 mmol) and 1 mL of zinc amalgam were stirred for 1 h under argon in 10 mL of C_6H_5Cl. The deep red solution of [Fe^{II}(TpivPP)] was then filtered into a second solution that was made by stirring for 2 h a mixture of 120 mg (0.319 mmol) of cryptand-222 and 190 mg of NaOCN (2.923 mmol) in 10 mL of C_6H_5Cl. The solution was filtered and crystals of the complex were prepared by slow diffusion of hexanes into the chlorobenzene solution. *Anal.* Calc. for **1** $C_{83}H_{100}FeN_{11}NaO_{11}$ (1506.60 g/mol): C, 66.17; H, 6.69; N, 10.23. Found: C, 66.28; H, 6.92; N, 10.35%. UV–Vis [C_6H_5Cl, λ_{max} in nm]: 437, 568, 610, 650. IR(KBr disk, cm^{-1}): ν(NCO): 2206.

2.3. Synthesis of [K(2,2,2-crypt)][Fe^{II}(TpivPP)(NCS)]·C_6H_5Cl (**2**)

Complex **2** was prepared by the procedures given for **1**, except that KSCN salt used instead of NaOCN. Good quality dark purple crystals of **2** were prepared by slow diffusion of hexanes into the C_6H_5Cl solution. *Anal.* Calc. for **2**, $C_{89}H_{105}ClFeKN_{11}O_{10}S$ (1651.25 g/mol): C, 64.74; H, 6.41; N, 9.33. Found: C, 64.82; H, 6.39; N, 9.57%. UV–Vis [C_6H_5Cl: λ_{max} in nm]: 436, 567, 612, 653. IR(KBr disk, cm^{-1}): ν(NCS): 2070, 2054.

2.4. X-ray crystallography

A single crystal of each compound was mounted under inert perfluoropolyether at the tip of glass fibre and cooled in the cryostream of a Bruker APEXII CCD diffractometer. Data for **1** and **2** were collected at 180 K using the monochromatic Mo Kα radiation (λ = 0.71073). The structures' solutions were obtained by direct method using SIR-2004-1.0 [5] and refined by full-matrix least-squares on $|F|^2$ using the SHELXL-97 program [6]. For complex **1** some disorder problems were encountered during the refinement of the structure: (i) the *tert-butyl* group of two pickets are disordered over two orientations (C40A–C41A–C42A/C40B–C41B–C42B and C62A–C63A–C64A/C62B–C63B–C64B) with refined occupancy coefficients converged to 0.674(7) and 0.326(7) (for the first *tert-butyl* group) and 0.846(6) and 0.154(6) (for the second *tert-butyl* group), (ii) three oxygen atoms of the TpivPP porphyrin are disordered in two positions: O1A/O1B, O3A/O3B and O4A/O4B with major positions occupancies of 0.54(12), 0.59(1) and 0.46(1), respectively, (iii) two oxygen atoms of one half cryptand-222 are also disordered in two positions with occupancies with the ratio of refined occu-

Table 1
Crystal data and refinement for **1** and **2**[a].

	1	**2**[a]
Empirical formula	$C_{83}H_{100}FeN_{11}NaO_{11}$	$C_{83}H_{100}FeKN_{11}O_{10}S$
Formula weight, (g mol)	1506.60	1538.78
Temperature (K)	180(2)	180(2)
Wavelength (Å)	0.71073	0.71073
Crystal system	Monoclinic	Monoclinic
Space group	C2	$P2_1/n$
a (Å)	24.0027(8)	18.1846(9)
b (Å)	14.7581(6)	21.5680(12)
c (Å)	23.6448(8)	22.6229(12)
β	106.078(2)	100.311(2)
V (Å^3)	8048.2(5)	8729.5(1)
Z	4	4
D_{calc} (g cm^{-1})	1.257	1.171
μ (mm^{-1})	0.260	0.304
F(0 0 0)	3236	3264
Crystal size (mm^3)	0.36 × 0.29 × 0.27	0.48 × 0.30 × 0.20
θ Range for data collection	2.60–26.37	2.06–26.02
Limiting indices	$-30 \leq h \leq 29$	$-22 \leq h \leq 22$
	$-18 \leq k \leq 18$	$-24 \leq k \leq 26$
	$-29 \leq l \leq 29$	$-27 \leq l \leq 27$
Completeness (%)	99.8	99.9
Absorption and minimum transmission	0.8931/1.0	0.8801/0.9892
Reflections collected/unique	64362/16382	127709/17182
R_{int}/R(σ)	0.0409/0.0447	0.0396/0.0342
Data/restraints/parameters	16382/498/1080	17182/18/969
Goodness-of-fit on F^2	1.024	1.106
Weights (w)	$[\sigma^2(F_o^2) + (0.0614P)^2 + 4.7845P]^{-1}$ $P = [\max(F_o^2, 0) + 2F_c^2]/3$	$[\sigma^2(F_o^2) + (0.1044P)^2 + 4.3502P]^{-1}$ $P = [\max(F_o^2, 0) + 2F_c^2]/3$
x (Flack parameter)	−0.027(11)	–
Final R indices [I > 2σ(I)]	R_1[b] = 0.0448, wR_2[c] = 0.1076	R_1[b] = 0.0562, wR_2[c] = 0.1669
R indices (all data)	R_1[b] = 0.0606, wR_2[c] = 0.1166	R_1[b] = 0.0771, wR_2[c] = 0.1803
Largest difference in peak and hole (e Å^{-3})	0.422 and −0.337	0.799 and −0.556

[a] Crystal data and refinement for **2** correspond to the complex with formula [K(2,2,2-crypt)][Fe^{II}(TpivPP)(NCS)]; the disordered chlorobenzene molecule was removed using the SQUEEZE option of the PLATON program.

[b] $R_1 = \Sigma||F_o| - |F_c||/\Sigma|F_o|$.

[c] $wR_2 = [\Sigma w(F_o^2 - F_c^2)^2/\Sigma w(F_o^2)^2]^{1/2}$.

pancies being 0.65(2):0.35(2) for O9A/O9B and 0.67(9):0.33(9) for O10A/O10B. The anisotropic displacement ellipsoids of some atoms of the porphyrin molecules and the counterions in complex **1** were very elongated which indicates static disorder. For fragments involving these atoms, the DFIX, DELU/SIMU and SIMU/ISOR restraints [7] and the EADP constraint commands in the SHELXL-97 [6] software were used which explains the huge number of restraints (Table 1). The TpivPP porphyrin of **2** also presents minor disorders: C29–C30–C31 (*s.o.f.* 0.863(4)/0.137(4)); C40–C41–C42 (*s.o.f.* 0.619(4)/0.381(4); O3 (*s.o.f.* 0.51(9)/0.49(9)). At the final stage of refinement of **2**, clear evidence of the presence of solvent voids of 189 Å^3 was obtained (containing approximately 46 electrons). Thus, a correction for diffuse effects due to the inclusion of the disordered chlorobenzene solvent in the crystal was made using the SQUEEZE subroutine in PLATON [8]. The absolute structure for **1** was set by reference to the Flack parameter equal to −0.027(11) [9]. For both complexes **1** and **2** non-hydrogen atoms were refined with anisotropic thermal parameters whereas H-atoms were included at estimated positions using a riding model. Drawings were made using ORTEP3 for windows [10]. Table 1 shows crystallographic data and structure refinement of complexes **1** and **2**. Selected bond distances and angles for these compounds are listed in Table 2.

Table 2
Selected bond distances (Å) and angles (°) in the molecular structures of [Na(2,2,2-crypt)][Fe^{II}(TpivPP)(NCO)] (complex **1**) and [K(2,2,2-crypt)][Fe^{II}(TpivPP)(NCS)] (complex **2**).

Complex **1**		Complex **2**	
Iron coordination polyhedron			
Fe–N1	2.107(2)	Fe–N1	2.103(2)
Fe–N2	2.128(2)	Fe–N2	2.106(2)
Fe–N3	2.111(2)	Fe–N3	2.093(2)
Fe–N4	2.134(2)	Fe–N4	2.116(2)
Fe–N9	2.005(3)	Fe–N9	2.042(2)
N9–Fe–N1	106.46(11)	N9–Fe–N1	107.06(10)
N1–Fe–N2	85.10(8)	N1–Fe–N2	87.16(8)
N1–Fe–N3	148.27(9)	N1–Fe–N3	153.07(8)
N1–Fe–N4	85.95(8)	N1–Fe–N4	85.48(8)
N2–Fe–N3	85.79(9)	N2–Fe–N3	87.38(8)
N2–Fe–N4	146.84(9)	N2–Fe–N4	152.25(8)
N3–Fe–N4	85.27(8)	N3–Fe–N4	87.18(8)
Cyanato-N ligand		*Thiocyanato-N ligand*	
N9–C65	1.151(4)	N9–C65	1.166(4)
C65–O5	1.197(4)	C65–S	1.639(3)
Fe–N9–C65	176.8(3)	Fe–N9–C65	170.2(3)
N9–C65–O5	179.8(6)	N9–C65–S	178.5(3)
Sodium-cryptand-222		*Potassium-cryptand-222*	
Na1–N10	2.701(3)	K–N10	3.058(2)
Na1–O6	2.462(2)	K–N11	3.036(3)
Na1–O7	2.540(3)	K–O5	2.827(2)
Na1–O8	2.519(3)	K–O6	2.808(2)
N10–Na1–O6	68.86(7)	K–O7	2.827(2)
N10–Na1–O7	67.66(9)	K–O8	2.857(2)
N10–Na1–O8	69.14(9)	K–O9	2.803(2)
O6–Na1–O7	107.29(9)	K–O10	2.864(2)
O6–Na1–O8	106.73(9)	N10–K–N11	179.76(8)
O7–Na1–O8	108.24(8)	O5–K–O6	60.50(7)
Na2–N11	2.911(4)	O8–K–O10	134.39(6)
Na2–O9A	2.416(7)	O9–K–O10	60.04(6)
Na2–O9B	2.676(13)	N10–K–O5	60.19(6)
Na2–O10A	2.633(5)	N10–K–O8	59.65(6)
Na2–O10B	2.469(10)	N10–K–O10	119.39(6)
Na2–O11	2.494(5)	N11–K–O6	59.68(8)
N11–Na2–O9A	65.1(2)	N11–K–O7	60.42(7)
N11–Na2–O9B	57.8(3)	N11–K–O9	120.50(7)
N11–Na2–O10A	62.92(15)		
N11–Na2–O10B	65.0(3)		
N11–Na2–O11	64.98(13)		
O9A–Na2–O10A	87.5(3)		
O9B–Na2–O10B	113.0(4)		
O9A–Na2–O11	102.9(3)		
O9B–Na2–O11	86.0(5)		
O10A–Na2–O11	115.20(15)		
O10B–Na2–O11	99.6(3)		

3. Results and discussion

3.1. UV–Vis and IR

The UV–Vis spectra of complexes **1** and **2** are very similar. They exhibit red shifted Soret bands at ~436 nm which is the case for Fe(II) five-coordinated *meso*-porphyrin complexes with anionic axial ligands (see Table 3). So, the electronic spectra of the pseudohalide NCS$^-$ and NCO$^-$ derivatives alone suggest the formation of a five-coordinated iron(II) porphyrin species. As shown in Table 3, the high-spin ($S = 2$) Fe(II) chloro, azido and oxyanionic (RO$^-$) species have Soret maxima around 440 nm [11]. Interestingly, however, the Soret maxima for five-coordinated low-spin ($S = 0$) iron(II) porphyrinates [Fe^{II}(TpivPP)(NO$_2$)]$^-$ [12] and [Fe^{II}(TpivPP)(CN)]$^-$ [13] are also in the 435–450 nm area.

Both **1** and **2** show a strong band in the IR spectra near 1102 cm^{-1} attributed to the C–O stretching frequencies of the cryptand-222. Complex **1** exhibits a strong absorption band at 2206 cm^{-1} attributed to the CN stretching frequency of the OCN$^-$ axial ligand which show clearly that the cyanato group is *N*-bound to the iron(II) ion [17]. The iron(III) analogue complex [Fe^{III}(TpivPP)(NCO)] [18], presents two absorption bands, assigned to

Table 3
Electronic spectra data[a] for selected iron(II) picket fence porphyrin complexes.

Complex	λ_{max} (nm)			Spin S	References
	Soret region	α, β region			
[Fe^{II}(TpivPP)(NCO)]$^-$	437	568	610	2	This work
[Fe^{II}(TpivPP)(NCS)]$^-$	436	567	612	2	This work
[Fe^{II}(TpivPP)(N$_3$)]$^-$	443	572	612	2	[14]
[Fe^{II}(TpivPP)(Cl)]$^-$	446	571	609	2	[15]
[Fe^{II}(TpivPP)(OMe)]$^-$	456	580	622	2	[11]
[Fe^{II}(TpivPP)(OAc)]$^-$	448	572	611	2	[11]
[Fe^{II}(TpivPP)(NO$_3$)]$^-$	438	564	604	2	[16]
[Fe^{II}(TpivPP)(NO$_2$)]$^-$	444	567	608	0	[12]
[Fe^{II}(TpivPP)(CN)]$^-$	455	565	601	0	[13]

[a] Solvent: chlorobenzene.

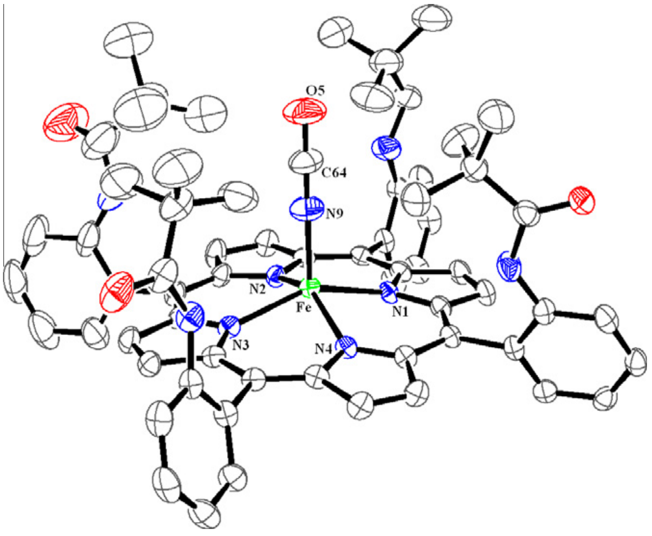

Fig. 1. ORTEP view of the ion complex [Fe^{II}(TpivPP)(NCO)]$^-$, thermal ellipsoids are drawn at the 50% probability level. Hydrogen atoms have been omitted for clarity.

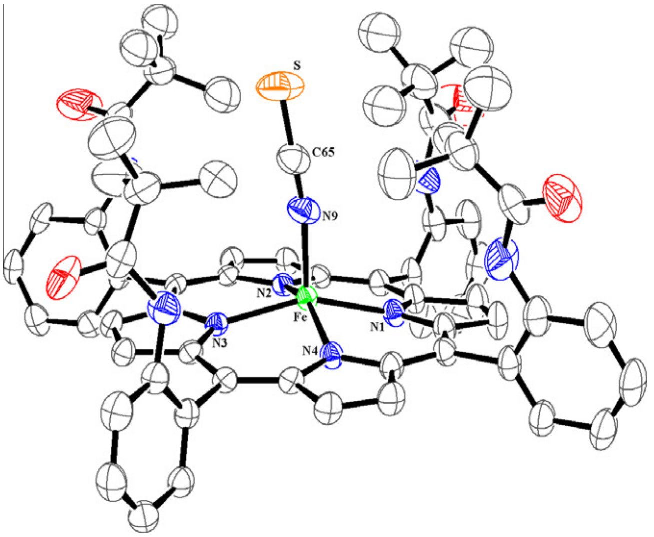

Fig. 2. ORTEP view of the ion complex [Fe^{II}(TpivPP)(NCS)]$^-$, thermal ellipsoids are drawn at the 50% probability level. Hydrogen atoms have been omitted for clarity.

the axial ligand, at lower frequencies (2200 and 2191 cm^{-1}). Complex **2** shows two strong absorption bands at 2070 and 2054 cm^{-1} attributed to the CN stretching frequencies of the thiocyanato-*N* ligand (denoted ν_{as} (NCS)) which are at higher energy than the one of the iron(III) derivative [Fe^{III}(TpivPP)(NCS)] [19] (2015 cm^{-1}).

3.2. Structural properties of [Na(2,2,2-crypt)][Fe^{II}(TpivPP)(NCO)] (complex 1) and [K(2,2,2-crypt)][Fe^{II}(TpivPP)(NCS)] (complex 2)

The asymmetric unit of **1** contains one ion complex [Fe^{II}(TpivPP)(NCO)]$^-$ and two half crystallographically independent counterions [Na(2,2,2-crypt)]$^+$ where each Na$^+$ occupies a special position on a two-fold axis. For complex **2** the asymmetric unit is made of one ion complex [Fe^{II}(TpivPP)(NCS)]$^-$, one [K(2,2,2-crypt)]$^+$ counterion and one chlorobenzene solvent molecule. For both complexes **1** and **2**, the iron(II) is coordinated to the four nitrogens of the porphyrin ring and the nitrogen atom of the pseudo-halide axial ligand from the pocket side of the TpivPP porphyrin. Figs. 1 and 2 are ORTEP drawings of the ionic complexes [Fe^{II}(TpivPP)(NCO)]$^-$ and [Fe^{II}(TpivPP)(NCS)]$^-$, respectively. As a consequence of the decreased charge, there is a small increase in

Table 4
Porphyrinato core parameters (Å) for selected five-coordinated iron(II) and iron(III) high-spin *meso*-porphyrin complexes.

Complex	Fe–N$_p$^{a}	Fe–X$_L$^{b}	Fe–P$_C$^{c}	Fe–P$_N$^{d}	References
Iron(II) high-spin porphyrins					
[Fe^{II}(TpivPP)(Cl)]$^-$	2.108(15)	2.301(2)	0.59	0.53	[3]
[Fe^{II}(TpivPP)(OAc]$^-$	2.107(2)	2.034(3)	0.64	0.55	[11]
[Fe^{II}(TpivPP)(NCO)]$^-$	2.120(2)	2.005(3)	0.6805(7)	0.5922(7)	This work
[Fe^{II}(TpivPP)(NCS)]$^-$	2.104(2)	2.042(2)	0.5923(12)	0.4965(9)	This work
[Fe^{II}(TpivPP)(η^1-ONO$_2$)]$^-$	2.070(16)	2.069(4)	0.49	0.42	[16]
[Fe^{II}(TpivPP)(N$_3$)]$^-$	2.094(3)	2.078(2)	0.525	0.459	[14]
Iron(III) high-spin porphyrins					
[Fe^{III}(TPP)(Cl)]	2.070(9)	2.211(1)	0.57	0.383(5)	[25]
[Fe^{III}(TPP)(I)]	2.066(11)	2.554(3)	0.53	–	[26]
[Fe^{III}(TTP)(OAc)]^e	2.067(4)	1.898(4)	0.520(1)	0.485(1)	[27]
[Fe^{III}(TpivPP)(NCO)]	2.069(5)	1.970(5)	0.540(1)	0.486(1)	[18]
[Fe^{III}(TpivPP)(NCS)]	2.055(2)	1.956(5)	0.504	0.462	[19]

[a] Average equatorial iron–nitrogen pyrrole distance.
[b] Iron–axial ligand distance.
[c] Distance between the iron atom and the mean plane made by the 24-atom core of the porphyrin.
[d] Distance between the iron center and the mean plane of the four pyrrole N atoms.
[e] TTP = tetratoluylporphyrin.

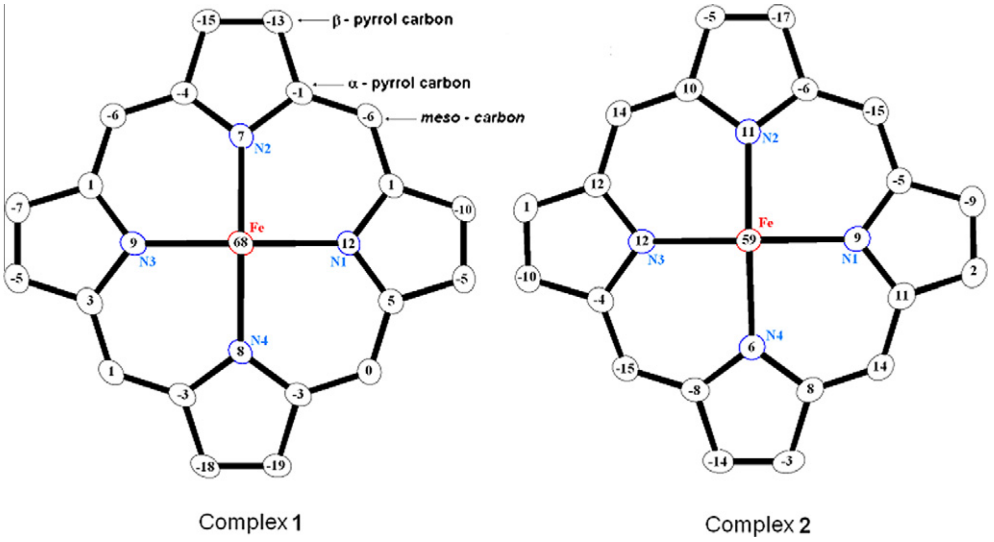

Fig. 3. ORTEP diagrams of the porphyrinato cores of the NCO derivative (left) and the NCS derivative (right). Shown are the perpendicular displacements, in units of 0.01 Å, from the 24-atom mean plane of the porphyrinato core. Positive values of displacement are toward the pseudo-halide ligands.

the radius of Fe^{2+} compared to Fe^{3+}, and this leads to increased bond lengths in the coordination group. Thus, the axial Fe^{II}–N(NCO) and Fe^{II}–N(NCS) bond lengths (2.005(3) Å and 2.042(2) Å, respectively) are longer than of the correspondent distances in the iron(III) derivatives [Fe^{III}(TpivPP)(NCO)] [18] and [Fe^{III}(TpivPP(NCS)] [19] (1.970(5) and 1.956(5) Å, respectively).

The NCO and the NCS groups are linear; the N9–C65–O5 bond angle is 179.8(6)° and the N9–C65–S bond angle is 178.5(3)°. For the NCO derivative N9–C65 and C65–O5 distances are 1.151(4) Å and 1.197(4) Å, respectively while for the NCS species, N9–C65 and C65–S distances are 1.166(4) Å and 1.639(3) Å, respectively. All these distances are in agreement with the literature values [20,21].

The deviation from a linear coordination of the axial ligand to the 24-atom core is more greater for the NCO ligand, i.e. Fe–N9–C65 bond angles are 176.8(3)° for **1** and 170.2(3)° for **2**. The average equatorial Fe–N$_p$ distances for the [Fe^{II}(TpivPP)(NCO)]$^-$ and [Fe^{II}(TpivPP)(NCS)]$^-$ ions complexes are 2.120(2) Å and 2.104(2) Å, respectively, are in the upper limit of the range (2.072–2.115 Å) [22] found for five-coordinated high-spin iron(II) porphyrinates. This is a stereochemical proof that complexes **1** and **2** are high-spin ($S = 2$). One can notice that these values are larger than those in the related Fe(III) species [Fe^{III}(TpivPP)(NCO)] [18] and [Fe^{III}(TpivPP)(NCS)] [19] (2.069(5) Å and 2.055(2) Å, respectively). In order to accommodate the high-spin iron(II) ion, the porphyrinato cores undergo a significant radial expansion. This is very well illustrated by the long Fe–P$_C$ = plane made by the 24-atom core of the porphyrin) and Fe–P$_N$ (P$_N$ = plane made by the four nitrogens of the porphyrin ring) distances shown by Fe(II) high-spin [Fe^{II}(Porph)(X)]$^-$ complexes (X is an anionic ligand). The values of Fe–P$_C$ distance for the iron(II) cyanato-*N* and thiocyanato-*N* species (0.6805(7) Å and 0.5923(12) Å, respectively) and for other five-coordinated iron porphyrinates are summarized in Table 4. We also notice that the Fe–P$_C$ and Fe–P$_N$ distances for **1** are the longest among all iron(II) species cited in Table 4. Illustrated in Fig. 3 are formal diagrams of the porphyrinato cores of **1** and **2**. Given are the displacements of each atom from the mean plane of the 24-atom porphyrin macrocycle in units of 0.01 Å. These diagrams show (i) **1** and **2** present a large domed deformation of the $C_{20}N_4$ least-squares plane as indicated by the values of the displacements of the nitrogen atoms toward the axial ligand, (ii) a ruffling distortion is quite significant for **2** as indicated by the displacement of the *meso* carbons above and below the porphyrin mean plane, (iii) complex **1** exhibits a moderate *S*4 saddle distortion of the 24-atom mean plane as mentioned by Scheidt and Lee [23]. The structural decomposition method (*NSD*) provided by Shelnutt and co-workers [24] indicated also a major doming deformation: dom = 0.349 Å (~56%) and a moderate saddle deformation: sad = 0.154 Å (~25%) for **1**, a major ruffling: ruf = 0.396 Å (~48%) and a moderate doming: dom = 0.281 Å (~34%) for **2**.

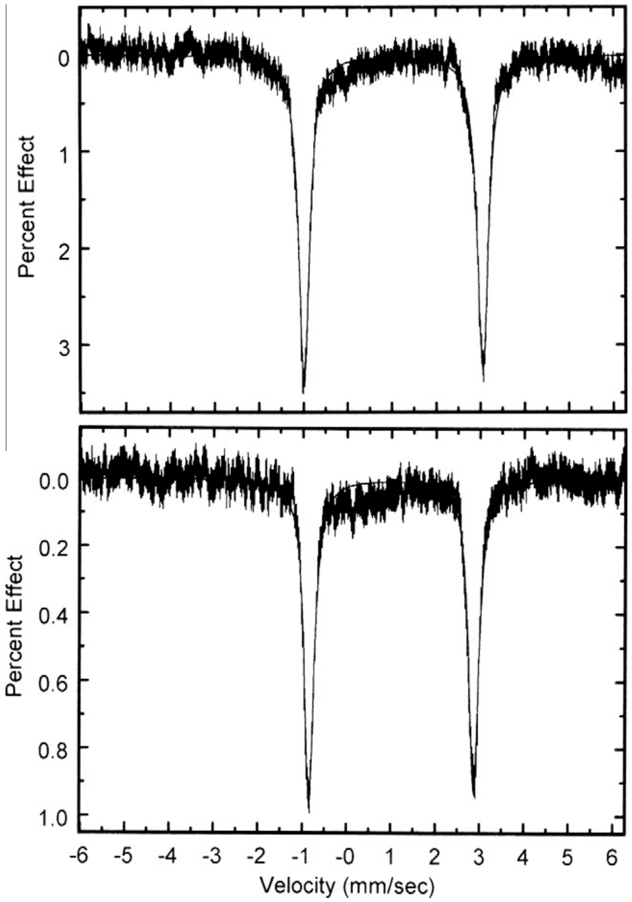

Fig. 4. Mössbauer spectra of **1** (top) and **2** (bottom) at 100 K in a weak applied magnetic field of 500 G. The solid lines are Lorentz fits to the data.

Table 5
Mössbauer parameters for some five-coordinated high-spin ($S = 2$) iron(II) picket fence porphyrin complexes.

Complex	ΔE_q (mm/s)	δ_{Fe} (mm/s)	T (K)	References
[Fe^{II}(TpivPP)(Cl)]$^-$	4.36	1.01	77	[3]
[Fe^{II}(TpivPP)(OMe)]$^-$	3,64	1.00	77	[11]
[Fe^{II}(TpivPP)(OAc)]$^-$	4.19	1.03	77	[11]
[Fe^{II}(TpivPP)(NO$_3$)]$^-$	3.59	0.98	77	[16]
[Fe^{II}(TpivPP)(N$_3$)]$^-$	4.23(1)	1.08(1)	20	[14]
[Fe^{II}(TpivPP)(NCO]$^-$	4.040(4)	1.042(4)	25	This work
	4.030(3)	1.043(3)	50	
	4.007(3)	1.032(3)	100	
[Fe^{II}(TpivPP)(NCS)]$^-$	3.720(5)	1.012(5)	25	This work
	3.739(6)	1.015(6)	50	
	3.694(7)	1.014(7)	100	

3.3. Mössbauer spectrum

The Mössbauer spectra of **1** and **2** are shown in Fig. 4 and isomer shift (δ_{Fe}) and quadrupole splitting (ΔE_q) values are given in Table 5 a-long with some comparative five-coordinated ferrous high-spin ($S = 2$) porphyrin species. As seen in this figure, the ΔE_q and δ_{Fe} values of the iron(II) porphyrinate derivatives **1** and **2** did not change too much with the temperature in range [25–100 K]. Metalloporphyrins with isomer shift values of ~1.00 mm/s are expected for high-spin iron(II) [28]. Indeed, the isomer shift values for **1** and **2** of 1.042(4) and 1.012(5) mm/s at 25 K, respectively strongly support a high-spin state assignment for these species. It has been notice by Schulz and co-workers [29] that five-coordinated high-spin iron(II) porphyrinates with anionic axial ligand (see Table 5) have distinctively large quadrupole splitting values ($\Delta E_q \sim 3.5$–4.5 mm/s). Indeed, the ΔE_q values are 4.040(4) and 3.720(5) mm/s (at 25 K) for **1** and **2**, respectively, which is consistent with their findings. These large quadrupole spittings values arise from a significant bonding orbital contribution to the electric-field gradient from the anionic axial ligand and that d_{xy} becomes the lowest d orbital in energy and hence, doubly occupied. We believe that the electronic repulsion of the iron(II) in-plane d_{xy} orbital by the negative charge of the pyrrole nitrogens is thus expected to increase the magnitude of the iron atom displacement from the porphyrin plane with a concomitant increase in the values of the Fe—N$_p$, Fe—P$_C$ and Fe—P$_N$ distances as is observed for our pseudo-halides iron(II) porphyrin derivatives.

4. Conclusion

Two new five-coordinated iron(II) porphyrinates [Na(2,2,2-crypt)] [Fe^{II}(TpivPP)(NCO)] (**1**) and [K(2,2,2-crypt)][Fe^{II}(TpivPP)(NCS)] (**2**) (TpivPP = α,α,α,α-tetrakis(*o*-pivalamidophenyl)porphyrin) were prepared and characterized by UV–Vis and IR spectroscopies. Structural and Mössbauer results are consistent with a high-spin ($S = 2$) state character of these two iron(II) pseudo-halide derivatives with a $(d_{xy})^2(d_{xz})^1(d_{yz})^1(d_{z^2})^1(d_{x^2-y^2})^1$ ground state electronic configuration. This investigations confirm the fact that for five-coordinated high-spin iron(II) porphyrinates type $[Fe(TpivPP)(X)]^-$, the large quadrupole splitting values are structurally related to the large iron(II) out-of-plane displacement and the concomitant long Fe–N_p bond lengths.

Acknowledgement

The authors gratefully acknowledge financial support from the Ministry of Higher Education and Scientific Research of Tunisia.

Appendix A. Supplementary material

CCDC 773788 and 773789 contains the supplementary crystallographic data for **1** and **2**. These data can be obtained free of charge from The Cambridge Crystallographic Data Centre via www.ccdc.cam.ac.uk/data_request/cif. Supplementary data associated with this article can be found, in the online version, at doi:10.1016/j.ica.2010.05.058.

References

[1] G. Simonneux, P. Le Maux, in: K.L. Kadish, K.M. Smith, R. Guilard (Eds.), The Porphyrin Handbook, vol. 11, Academic Press, 2000, p. 133.
[2] (a) C. Hu, A. Roth, M.K. Ellison, J. An, C.M. Ellis, C.E. Schulz, W.R. Scheidt, J. Am. Chem. Soc. 127 (2005) 5675;
(b) C. Hu, C.D. Sulok, F. Paulat, N. Lehnert, A.I. Twigg, M.P. Hendrich, C.E. Schulz, W.R. Scheidt, J. Am. Chem. Soc. 132 (2010) 3737.
[3] M. Schappacher, Ph.D. Thesis, Université Louis Pasteur, Strasbourg, France, 1982.
[4] A. Gismelseed, E.I. Bill, A.X. Trautwein, H. Winkler, H. Nasri, P. Doppelt, D. Mandon, J. Fischer, R. Weiss, Inorg. Chem. 29 (1990) 2741.
[5] M.C. Burla, R. Caliandro, M. Camalli, B. Carrozzini, G.L. Cascarano, L. De Caro, C. Giacovazzo, G. Polidori, R. Spagna, J. Appl. Cryst. 38 (2005) 381.
[6] G.M. Sheldrick, Acta Crystallogr., Sect. A 64 (2008) 112.
[7] P. McArdle, J. Appl. Cryst. 28 (1995) 65.
[8] A.L. Spek, Acta Crystallogr., Sect. D 65 (2009) 148.
[9] H.D. Flack, G. Bernardinelli, J. Appl. Cryst. 33 (2000) 1143.
[10] L.J. Farrugia, J. Appl. Cryst. 30 (1997) 565.
[11] H. Nasri, J. Fischer, R. Weiss, J. Am. Chem. Soc. 109 (1987) 2549.
[12] H. Nasri, M.K. Ellison, C. Krebs, B.H. Huynh, W.R. Scheidt, J. Am. Chem. Soc. 122 (2000) 10795.
[13] H. Ben Abbes, H. Nasri, unpublished results.
[14] I. Hachem, M.S. Belkhiria, M. Giorgi, C.E. Schulz, H. Nasri, Polyhedron 28 (2009) 954.
[15] M. Schappacher, L. Ricard, R. Weiss, Inorg. Chem. Acta (1983) L9.
[16] H. Nasri, M.K. Ellison, B. Shaevitz, G.P. Gupta, W.R. Scheidt, Inorg. Chem. 45 (2006) 5284.
[17] K. Nakamoto, Infrared and Raman Spectra of Inorganic and Coordination Compounds, Part B, 6th ed., John Wiley and Sons, New York, 2009.
[18] M.S. Belkhiria, M. Dhifet, H. Nasri, J. Porphyrins Phthalocyanines 9 (2005) 575.
[19] H. Nasri, M. Debbabi, Polyhedron 17 (1998) 3607.
[20] A.K. Boudalis, J.-M. Clemente-Juan, F. Dahan, J.-P. Tuchagues, Inorg. Chem. 43 (2004) 1574.
[21] C.J. Siemer, F.A. Meece, W.H. Armstrong, D.M. Eichhorn, Polyhedron 20 (2001) 2637.
[22] (a) W.R. Scheidt, C.A. Reed, Chem. Rev. 81 (1981) 543;
(b) W.R. Scheidt, in: K.L. Kadish, K.M. Smith, R. Guilard (Eds.), The Porphyrin Handbook, vol. 3, Academic Press, 2000, p. 49.
[23] W.R. Scheidt, Y. Lee, Struct. Bond. (Berlin) 64 (1987) 1.
[24] W. Jensen, J.-G. Ma, J.A. Shelnutt, J. Biophys. 74 (1998) 753.
[25] H. Nasri, Ph.D. Thesis, Universite Louis Pasteur, Strasbourg, France, 1987.
[26] K. Hatano, W.R. Scheidt, Inorg. Chem. 18 (1979) 877.
[27] H. Oumous, C. Lecomte, J. Protas, P. Cocolios, R. Guilard, Polyhedron 3 (1984) 651.
[28] P.G. Debrunner, in: A.B.P. Lever, H.B. Gray (Eds.), Iron Porphyrin Part 3, Academic Press, New York, 1983 (Chapter 2).
[29] C. Hu, B.C. Noll, C.E. Schulz, W.R. Scheidt, J. Am. Chem. Soc. 127 (2005) 15018.